Step-position distributions and the pairwise Einstein model for steps on crystal surfaces

Amber N. Benson,[1,2,*] Howard L. Richards,[2,†] and T. L. Einstein[3,‡]

[1]*Department of Physics and Astronomy, Mississippi State, Mississippi 39762-5167, USA*
[2]*Department of Physics, Texas A & M University–Commerce, Commerce, Texas 75429-3011, USA*
[3]*Department of Physics, University of Maryland, College Park, Maryland 20742-4111, USA*

The pairwise Einstein model of steps not only justifies the use of the generalized Wigner distribution (GWD) for terrace width distributions (TWDs), it also predicts a specific form for the step position distribution (SPD), i.e., the probability density function for the fluctuations of a step about its average position. The predicted form of the SPD is well approximated by a Gaussian with a finite variance. However, the variance of the SPD measured from either real surfaces or Monte Carlo simulations depends on Δy, the length of step over which it is calculated, with the measured variance diverging in the limit $\Delta y \rightarrow \infty$. As a result, a length scale L_W can be defined as the value of Δy at which the measured and theoretical SPDs agree. Monte Carlo simulations of the terrace-step-kink model indicate that $L_W \approx 14.2 \xi_Q$, where ξ_Q is the correlation length in the direction parallel to the steps, independent of the strength of the step-step repulsion. L_W can also be understood as the length over which a *single* terrace must be sampled for the TWD to bear a "reasonable" resemblence to the GWD.

I. INTRODUCTION

A key factor determining the equilibrium morphology of a vicinal crystal surface is the interaction between the steps on that surface. In many cases, the elastic and electronic contributions to the step-step interaction take the form

$$V(L) = \frac{A}{L^2},\qquad(1)$$

where A determines the strength of the step-step interaction and L is the distance between steps. Because this is a typical step-step interaction, and because it has the remarkable property of yielding exact solutions to very plausible approximate theories,[1–3] we confine ourselves in this paper to interactions of the form given in Eq. (1). With this restriction, many of the quantities discussed in this paper depend only on a single dimensionless parameter

$$\widetilde{A} \equiv \frac{\widetilde{\beta} A}{(k_B T)^2},\qquad(2)$$

where $\widetilde{\beta}$ is the step stiffness, k_B is Boltzmann's constant, and T is the absolute temperature.

One of the easiest methods[4–6] for experimentally determining the interaction between steps on a vicinal crystal surface is through the observation of the terrace width distribution (TWD). Typically, this has been done by fitting the TWD to a Gaussian, which is a good approximation and justified by the Gruber-Mullins approximation[7,8] (analogous to the Einstein model[9] of solids) if the steps strongly repel each other. The step-step interaction is then extracted from the variance of the Gaussian. Unfortunately, however, the Gaussian approximation is only good for strongly interacting steps, and there are conflicting theories[7,8,10–14] regarding the relationship between the step-step interaction and the variance.

Over the past decade[4–6] it has become apparent that the so-called generalized Wigner distribution (GWD) provides a much better approximation to the TWD. The GWD exhibits the positive skew observed in TWDs from experiments and simulations, and it is a good fit quantitatively to TWDs produced from Monte Carlo simulations of the terrace-step-kink (TSK) model. More significantly, the GWD can be justified on the basis of plausible approximations,[3,15] the most important of which is that the interaction and fluctuations of *two* adjacent steps are explicitly considered; the Gruber-Mullins approximation only explicitly considers *one* step. The two steps are kept close to each other by a harmonic well, which approximates the interactions with all other steps. This model is referred to as the pairwise Einstein model (PEM). Both the Gruber-Mullins and PEMs start by interpreting the steps as world-lines of spinless fermions, with the y direcion (the average direction of the steps) corresponding to time.

This paper considers a different statistical measure of the vicinal surface: the step position distribution (SPD). In Sec. II, we show that the PEM predicts a Gaussian-like distribution for the position of steps. In Sec. III these predictions are shown to compare well with numerical results from simulations of the TSK model, at least for systems of the "right size." The dependence of the SPD on the length of the steps is discussed in Sec. IV; for the purpose of comparison, the dependence of the TWD on the length of steps is likewise discussed in Sec. V. Finally, in Sec. VI we summarize and draw our conclusions.

II. PREDICTIONS FROM THE PAIRWISE EINSTEIN MODEL

As was shown in Ref. 3, the GWD can be derived from a phenomenological treatment in which only two steps are treated explicitly, the rest contributing a "confinement potential" related to the two-dimensional pressure and compressibility of the system of steps. We use the usual trick of map-

ping steps onto the worldlines of one-dimensional spinless fermions, which in this case have the Hamiltonian[3,15]

$$\mathcal{H} = -\frac{1}{2}\left(\frac{\partial^2}{\partial x_1^2} + \frac{\partial^2}{\partial x_2^2}\right) + \frac{\tilde{A}}{(x_2 - x_1)^2} + \frac{\omega^2}{2}(x_1^2 + x_2^2). \quad (3)$$

In this dimensionless formulation, we require that

$$\langle x_2 - x_1 \rangle = 1; \quad (4)$$

this fixes the value of ω to

$$\omega = 2b_\varrho, \quad (5)$$

where

$$b_\varrho \equiv \left[\frac{\Gamma\left(\frac{\varrho + 2}{2}\right)}{\Gamma\left(\frac{\varrho + 1}{2}\right)}\right]^2 \quad (6)$$

and

$$\varrho = 1 + \sqrt{1 + 4\tilde{A}}. \quad (7)$$

After a change of variables[3,15] to

$$x_{\text{c.m.}} = \frac{x_1 + x_2}{2}, \quad (8)$$

$$s = x_2 - x_1, \quad (9)$$

this Hamiltonian becomes separable,[3,15]

$$\mathcal{H} = -\left(\frac{\partial^2}{\partial s^2} + \frac{1}{4}\frac{\partial^2}{\partial x_{\text{c.m.}}^2}\right) + \frac{\tilde{A}}{s^2} + b_\varrho^2(s^2 + 4x_{\text{c.m.}}^2), \quad (10)$$

and it has the remarkable property that all of the eigenstates are known. The only eigenstate of interest to us at present, however, is the ground state, which can be written[3,15]

$$\Psi_{0,0}(s, x_{\text{c.m.}}) = \left[a_\varrho^{1/2} s^{\varrho/2} \exp\left(-\frac{b_\varrho s^2}{2}\right)\right]$$

$$\times \left[\frac{1}{2\sqrt{\pi b_\varrho}} \exp(-4b_\varrho x_{\text{c.m.}}^2)\right], \quad (11)$$

where

$$a_\varrho = \frac{2b_\varrho^{(\varrho+1)/2}}{\Gamma[(\varrho + 1)/2]} \quad (12)$$

is a constant of normalization. The probability of finding a specific combination of relative separation and "center of mass" is, of course, just $\Psi_{0,0}^2(s, x_{\text{c.m.}})$, which can be rewritten in terms of the original variables x_1 and x_2:

$$P(x_1, x_2) = \Psi_{0,0}^2(s, x_{\text{c.m.}}) = \frac{a_\varrho}{\sqrt{\pi b_\varrho}}(x_2 - x_1)^\varrho \exp[-2b_\varrho(x_1^2 + x_2^2)], \quad (13)$$

subject to the constraint $x_2 \geq x_1$. We can integrate out all possible values of x_2 to find the probability density function for x_1:

$$Q_1(x_1) = \int_{x_1}^\infty P(x_1, x_2)dx_2 = \frac{a_\varrho}{\sqrt{\pi b_\varrho}}\exp(-2b_\varrho x_1^2)$$

$$\times \int_{x_1}^\infty (x_2 - x_1)^\varrho \exp(-2b_\varrho x_2^2)dx_2. \quad (14)$$

As should be expected, the mean value of x_1 is $-1/2$ and the mean value of x_2 is $+1/2$, so we define the analytic SPD to be the calculated probability density function for $x_1 - \langle x_1 \rangle$:

$$Q(x) \equiv Q_1\left(x + \frac{1}{2}\right) = \frac{a_\varrho}{\sqrt{\pi b_\varrho}}\exp\left[-2b_\varrho\left(x + \frac{1}{2}\right)^2\right]$$

$$\times \int_x^\infty \left(x_2 - x + \frac{1}{2}\right)^\varrho \exp(-2b_\varrho x_2^2)dx_2. \quad (15)$$

Although $Q(x)$ can only be evaluated numerically (it can be rewritten as a complicated expression involving hypergeometric functions, but this does not seem to be genuinely helpful), it is straightforward, though tedious, to calculate its moments. The two most important are the mean, which is zero by definition, and the variance, which is given by

$$\sigma_{Q,W}^2 = \frac{1}{4}\left(\frac{\varrho + 2}{2b_\varrho} - 1\right) \quad (16)$$

$$\sim \frac{3}{8}\varrho^{-1}. \quad (17)$$

These two moments would be enough to entirely specify the SPD if it were a Gaussian distribution, which it should be approximately; the Gruber-Mullins approximation for the TWD, since it concerns the fluctuations in position of only a single step, can be equally well interpreted as an approximation for the SPD. In fact, both the coefficient of skewness[16] and the kurtosis[16] of the theoretical SPD vanish in the limit of strong step-step repulsion. The coefficient of skewness is given asymptotically by

$$\gamma_1 \equiv \frac{\langle (x_1 - \langle x_1 \rangle)^3 \rangle}{\sigma_{Q,W}^3} \sim -\frac{\sqrt{6}}{18}\varrho^{-1/2}; \quad (18)$$

note that the coefficient of skewness would have the opposite sign if it had been defined as $\langle (x_2 - \langle x_2 \rangle)^3 \rangle \sigma_{Q,W}^{-3}$. The kurtosis, which is the same regardless of which step is considered, is given asymptotically by

$$\gamma_2 \equiv \frac{\langle (x_1 - \langle x_1 \rangle)^4 \rangle}{\sigma_{Q,W}^4} - 3 \sim \frac{1}{12}\varrho^{-2}. \quad (19)$$

The fact that the kurtosis is not exactly zero is not in itself surprising; even within the Gruber-Mullins approximation, the Gaussian distribution is only obtained in the limit of large $\tilde{A}$. The symmetry of our original problem of an infinite number of steps on an infinite vicinal surface, on the other hand, means that the coefficient of skewness, by contrast, *must* be zero for the original problem. Any given step on the surface can be considered "step 1," with its downhill neighbor as "step 2," or it can be considered "step 2," with its uphill neighbor as "step 1;" calling it one or the other breaks the

symmetry and permits a nonzero coefficient of skewness.

III. COMPARISON WITH MONTE CARLO SIMULATIONS

In order to test the applicability of Eq. (15), we have performed Monte Carlo simulations of the TSK model and measured the SPD for several values of $\tilde{A}$.

The geometry of the simulated systems was as follows. All simulations were for systems of 30 steps; the length of each of which was $L_y = 1000a$ (where a is the lattice constant) in the average direction of the steps (the y direction in "Maryland notation"). The mean step separation was $\langle L \rangle = 10a$, and periodic boundary conditions were applied.

The dynamic used was a local Metropolis update. The temperature was set at $k_B T = 0.45\epsilon$, where ϵ is the kink energy; in a previous study,[22] this was approximately the temperature at which TWDs from the restricted TSK model showed the best agreement with the generalized Wigner distribution. Each simulation was equilibrated for at least 500 000 Monte Carlo steps per site (MCSS) at the temperature and value of $\tilde{A}$ at which measurements were taken; the initial configurations, however, were not typically straight steps, but steps that had been equilibrated at some other value of $\tilde{A}$. Data were taken from 1000 "snapshots," taken at intervals of 1000 MCSS.

Although the terrace width is always an integer multiple of a in the TSK model, the average step position can be any rational number, depending only on the size of the simulation. Since the step position x is always an integer, the histogram of positions for any given step need not be symmetric.

In order to show concretely what this means, consider a situation in which a Gaussian distribution with mean μ and variance σ^2 is binned into a histogram as follows. The weight assigned to each integer k is given by integrating the Gaussian between $k - 1/2$ and $k + 1/2$:
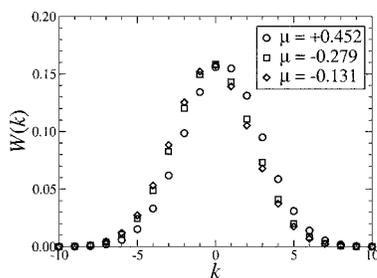
FIG. 1. An illustration of problem that can be caused by the variability of the mean step position when the SPD is calculated from numerical or experimental results. In this example, Gaussian distributions with identical variances ($\sigma^2 = 2.5^2$) are binned into histograms by means of Eq. (20). The only differences between the three distributions are the values of μ: circles, $\mu = 0.452$; squares, $\mu = -0.279$; diamonds, $\mu = -0.131$.
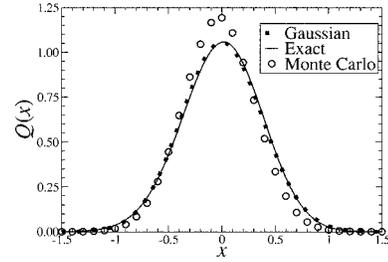
FIG. 2. Comparison of the SPD for $\tilde{A} = 0$ given by Eq. (15) (solid curve) with a histogram SPD from a Monte Carlo simulation (symbols). Also shown is a Gaussian (dotted curve) with a mean of zero and a variance given by Eq. (16).

$$W(k) = \frac{1}{\sigma\sqrt{2\pi}} \int_{k-1/2}^{k+1/2} \exp\left[-\frac{(x-\mu)^2}{2\sigma^2} \right] dx$$

$$= \frac{1}{2}\left\{ \text{erf}\left[\frac{k - (1/2) - \mu}{2\sigma} \right] - \text{erf}\left[\frac{k + (1/2) - \mu}{2\sigma} \right] \right\}.$$

(20)

For our example, we choose $\sigma = 2.5$ and three "random" values of μ between -0.5 and $+0.5$. The results are shown in Fig. 1. Clearly none of the histograms is completely symmetric, and the differences between them are noteworthy.

Something similar can and does happen when the SPDs are calculated from Monte Carlo simulations by binning the positions into histograms. As a result, the statistical uncertainties are considerably larger than they are for the corresponding TWDs, and the SPDs are not perfectly symmetric about their peaks, as can be seen in Figs. 2 and 3. Note the qualitative similarities between the Monte Carlo results (circles) in Figs. 2 and 3 and the values of $W(k)$ for $\mu = -0.279$ (squares) and $\mu = -0.131$ (diamonds) in Fig. 1. This agreement suggests that during the process of equilibration, the majority of the steps moved slightly to the left (i.e., uphill).

In spite of this, the agreement of the SPDs calculated from simulations and the theoretical $Q(x)$ calculated from Eq. (15) is reasonably good. Even more impressive is the agreement between $Q(x)$ and the Gaussian with zero mean and variance given by Eq. (16). Although Eqs. (18) and (19) suggest that the Gaussian approximation will be increasingly
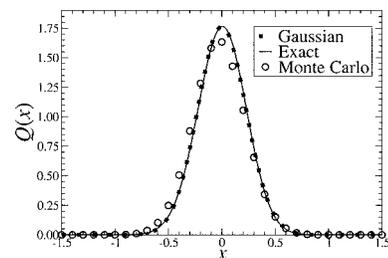
FIG. 3. Comparison of the SPD for $\tilde{A} = 8$ given by Eq. (15) (solid curve) with a histogram SPD from a Monte Carlo simulation (symbols). Also shown is a Gaussian (dotted curve) with a mean of zero and a variance given by Eq. (16).

good as $\widetilde{A}$ becomes large, it is clear from the figures that the Gaussian approximation is good even for $\widetilde{A}=0$.

IV. SCALING OF THE SPD

Although the agreement between Eq. (15) and the numerical SPDs discussed above is highly suggestive, it is clear that actual step position distributions must depend on the length Δy of step over which they are averaged. This is best demonstrated by considering the variance of a measured SPD, which is given by

$$\sigma_Q^2(\Delta y) \equiv (\Delta y) - 1 \left\langle \int_{-\Delta y/2}^{\Delta y/2} [x(y) - \bar{x}]^2 dy \right\rangle, \quad (21)$$

where

$$\bar{x} \equiv (\Delta y)^{-1} \int_{-\Delta y/2}^{\Delta y/2} x(y) dy. \quad (22)$$

Clearly, $\sigma_Q^2(\Delta y)$ is closely related to[17]

$$g_x(\Delta y) \equiv \langle [x(\Delta y) - x(0)]^2 \rangle, \quad (23)$$

which characterizes the wandering of an individual step.[17–21]

It is tempting to identify $\bar{x}$, the average value of x for a particular conformation of a step, with $x(0)$, the value of x at the average y position. This leads to

$$\sigma_Q^2(\Delta y) \approx (\Delta y)^{-1} \int_{-\Delta y/2}^{\Delta y/2} g_x(y) dy. \quad (24)$$

For small Δy, $g_x \approx c_1 |\Delta y|$;[17–21] Eq. (24) implies $\sigma_Q^2 \approx (c_1/2)\Delta y$. Likewise, for large Δy,[17–21]

$$g_x(\Delta y) \approx c_2 + c_3 ln|\Delta y| \quad (25)$$

and Eq. (24) implies

$$\frac{\sigma_Q^2(\Delta y)}{\sigma_{Q,W}^2} \approx c_4 + c_5 ln|\Delta y|. \quad (26)$$

The observation, made in the previous section, that $Q(x)$ is to a very good approximation Gaussian is helpful towards the calculation of the characteristic length for σ_Q^2. In Ref. 8, the "TWD" was calculated within the Gruber-Mullins approximation; because the position of only one step was explicitly taken into account, though, it could equally be considered a SPD. In fact, the Gaussian solution is a more appropriate description of a SPD, which is symmetric, than a TWD, which is asymmetric. Substituting the variance of the SPD into Eq. 18 of Ref. 8, we find the correlation length to be

$$\xi_Q = \frac{2\langle L \rangle^2 \widetilde{\beta} \sigma_{Q,W}^2}{k_B T}. \quad (27)$$

Figure 4 shows a comparison between ξ_Q and the correlation length from Ref. 8.

Scaled by $\sigma_{Q,W}^2$ and ξ_Q, $\sigma_Q^2(\Delta y)$ appears to be independent of $\widetilde{A}$; although the PEM incorrectly predicts that $\sigma_Q^2(\Delta y)$ re-
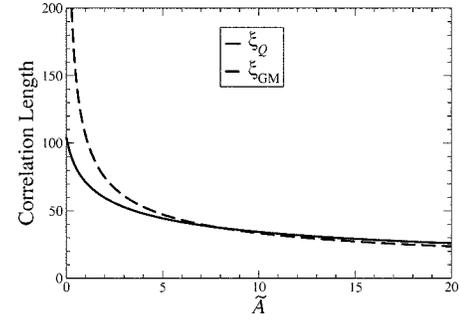
FIG. 4. Comparison of the correlation length calculated from the SPD (ξ_Q) and from the Gruber-Mullins approximation (ξ_{GM}), evaluated numerically for $\langle L \rangle = 10$ and $k_B T = 0.45\epsilon$. Although there is decent agreement for $\widetilde{A} > 5$, ξ_{GM} unphysically diverges as $\widetilde{A} \to 0$. In contrast, ξ_Q remains finite and reasonable for all nonnegative values of $\widetilde{A}$.

mains finite in the limit $\Delta y \to \infty$, it nevertheless provides the correct scaling factors. This is remarkable, since although $g_x(\Delta y)$ shows scaling with temperature, it does not exhibit scaling independent of $\widetilde{A}$.[17]

For $\Delta y < \xi_Q$, a least-squares fit indicates power-law growth of $\sigma_Q^2(\Delta y)$ with an exponent of 0.797 ± 0.006 (Fig. 5). Equation (24) predicts power-law growth, but with an exponent of 1. Interestingly, the power-law behavior of $g_x(\Delta y)$ extends only out to[17] $\Delta y \approx 0.1 y_{coll}$; since $y_{coll} = \xi_Q/(\pi-2)$ (for $\widetilde{A}=0$), power-law scaling extends farther for $\sigma_Q^2(\Delta y)$ than for $g_x(\Delta y)$.

For large Δy, $\sigma_Q^2(\Delta y)$ follows the logarithmic scaling of Eq. (26). A least-squares fit was performed on the $\widetilde{A}=8$ data, since this has the smallest value of ξ_Q among the available simulations, and hence the largest available values of $\Delta y/\xi_Q$. To avoid the crossover from the power-law regime, the fit was restricted to $\Delta y > 4\xi_Q$; likewise, the fit was limited to $\Delta y < L_y/2$ to limit finite-size effects. The resulting fit, shown in Fig. 6, is in good agreement with data from all values of $\widetilde{A}$ except where finite-size effects become evident. The fitted parameters $c_4 = 0.1578 \pm 0.0004$ and $c_5 = 0.3175 \pm 0.0002$ allow us to find a "Wigner length" L_W, defined by

$$\sigma_Q^2(L_W) \equiv \sigma_{Q,W}^2 \quad (28)$$

to be
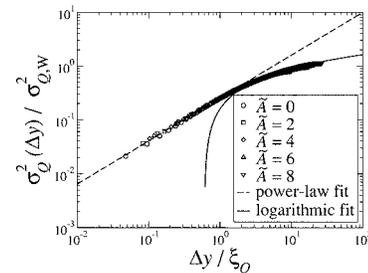
FIG. 5. A power-law fit to all the Monte Carlo estimates of $\sigma_Q^2(\Delta y)$ for $0 \le \widetilde{A} \le 8$, $\Delta y < \xi_Q$, indicates an initial growth with an exponent of 0.797 ± 0.006.
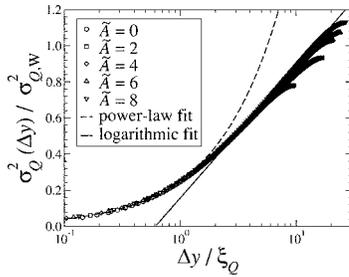
FIG. 6. A fit to the Monte Carlo estimates of $\sigma_Q^2(\Delta y)$ for $\tilde{A}=8$, $4\xi_Q < \Delta y < L_y/2$, indicates an asymptotic growth given by $\sigma_Q^2(\Delta y)/\sigma_{Q,W}^2 \approx 0.158 + 0.3175\ln(\Delta y/\xi_Q)$. The length L_W, defined by Eq. (28), $\sigma_Q^2(L_W) \equiv \sigma_{Q,W}^2$, is consequently given by $L_W = (14.183 \pm 0.035)\xi_Q$.

$$L_W = (14.183 \pm 0.035)\xi_Q. \qquad (29)$$

V. SCALING OF THE TWD

It seems somewhat surprising that so many correlation lengths are necessary for the PEM to agree with the observed variance. To better understand this, it is helpful to consider the corresponding scaling of the TWD when it is calculated under the same restrictions as $\sigma_Q^2(\Delta y)$. Specifically, the TWD must be averaged over a given length Δy of a single pair of adjacent steps in a single "snapshot." This is very different from the analysis presented in Ref. 22, where, as in other previous work, averages were made over the entire length L_y of the simulations, over all pairs of neighboring steps, and over all "snapshots." Remembering that the y direction corresponds to time in the worldline interpretation of steps, the averages we are about to calculate correspond to time averages in statistical mechanics, whereas the previous averages have combined the time average with two kinds of ensemble average (over different pairs and different "snapshots"). Only in the limits of long times and large ensembles should one expect these averages to be identical.[23]

In the language of Ref. 17, ξ_Q is approximately the distance between "collisions" of neighboring steps. In order to
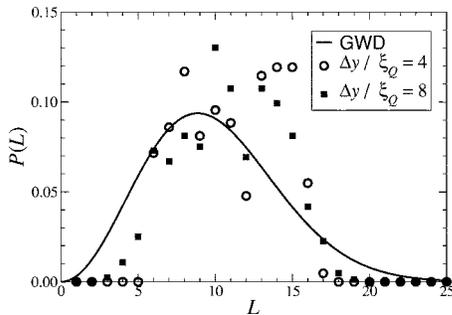
FIG. 7. Terrace width distributions calculated between a single pair of neighboring steps depend on Δy, the length of step over which the distribution is averaged. Although in the limit $\Delta y \to \infty$ the TWD converges to the GWD (to a very good approximation), when $\Delta y/\xi_Q$ is small the TWD is dominated by noise. These results are typical for $\tilde{A}=0$.
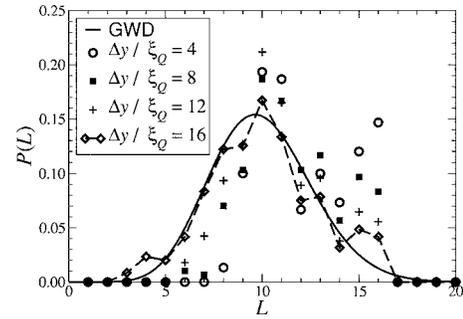
FIG. 8. For small $\Delta y/\xi_Q$, typical TWDs are dominated by noise, but for $\Delta y > L_W \approx 14.2\xi_Q$, the GWD dominates. These results are for $\tilde{A}=8$.

sample the distribution of terrace widths adequately, a step must "collide" several times with its neighbors. This is shown clearly in Figs. 7 and 8. For the simulation parameters given in Sec. III, $L_W > L_y$ for $\tilde{A}=0$; consequently, the TWDs shown in Fig. 7 are dominated by noise. For $\tilde{A}=8$, on the other hand, $L_W < L_y$, and we are able to see in Fig. 8 the crossover into the regime where the GWD, not noise, is dominant.

The role of step collisions in equilibrating the TWD can also be seen from $\sigma_P^2(\Delta y)$, which is the variance of TWDs calculated from a length Δy of neighboring steps, averaged over all pairs of neighboring steps, starting points, and "snapshots." As with $\sigma_Q^2(\Delta y)$, $\lim_{\Delta y \to 0}\sigma_P^2(\Delta y)=0$; unlike $\sigma_Q^2(\Delta y)$, $\lim_{\Delta y \to \infty}\sigma_P^2(\Delta y)$ is finite and given approximately[22] by the PEM result[24]

$$\sigma_{P,W}^2 = \frac{\varrho + 1}{2b_\varrho} - 1. \qquad (30)$$

This suggests plotting $1 - \sigma_P^2(\Delta y)/\sigma_{P,W}^2$ vs $\Delta y/\xi_Q$ to determine whether the approach to the asymptotic limit is exponential or power law. As shown in Fig. 9, the scaling appear to be neither a simple power law nor a simple exponential decay, but it is difficult to be certain since the TWD does not converge *exactly* to the GWD even in the limit $\Delta y \to \infty$. Also, the scaling does not appear to be quite as precise as in Figs. 5 and 6. This is not surprising, since the correlation length ξ_P for the TWD is not identical to ξ_Q.
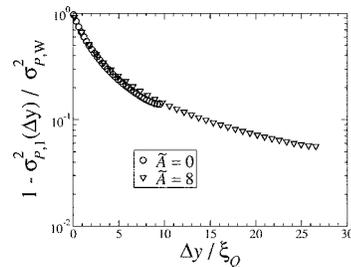
FIG. 9. The variance of the TWD also approximately scales with $\Delta y/\xi_Q$. At $\Delta y = L_W \approx 14.2\xi_Q$, the average variance of TWDs generated from single pairs of neighboring steps is within about 10% of the variance given by the GWD.

TABLE I. Asymptotic variances in the limit of strong step-step repulsion. The Gaussian-like approximation for the SPD given by Eq. (15) is compared with selected approximations for the TWD. Except for the GWD, all approximate TWDs are Gaussian approximations. Note also that our approximation for the SPD and the GWD are both independent of the number of interacting steps, whereas the Gaussian approximations are not. (See also Table I of Ref. 6.)

Distribution	Ref.	Asymptotic variance
SPD	Eq. (16)	$0.375\varrho^{-1}$
Generalized Wigner	24–26	$0.5\varrho^{-1}$
Gruber Mullins (all steps)	7	$0.278\varrho^{-1}$
Gruber Mullins (nearest neighbors)	7	$0.289\varrho^{-1}$
Modified Grenoble (all steps)	10, 11, and 24	$0.495\varrho^{-1}$
Modified Grenoble (nearest neighbors)	10, 11, and 24	$0.520\varrho^{-1}$
Saclay (all steps)	12–14	$0.405\varrho^{-1}$

More significantly, Fig. 9 indicates that $\sigma_P^2(L_W)$ is within about 10% of the approximate asymptotic value $\sigma_{P,W}^2$. This is a very plausible threshold for statistics from the TWD.

VI. CONCLUSION

For the common case in which steps on a vicinal crystal surface interact according to Eq. (1), the GWD has been shown previously to be in excellent agreement with the TWD. To fully appreciate the model which predicts the GWD, though, it is necessary to examine its predictions for other statistical properties and how well these predictions agree with actual measurements. This article has made such a comparison between the predicted and measured SPD. The results demonstrate both the strength and limitations of the PEM.

Since the SPD is so well approximated by a Gaussian, it is tempting to compare it directly with Gaussian theories of the TWD. As can be seen in Table I, in the limit of strongly interacting steps the variance of the SPD is slightly larger than that of the Gruber-Mullins approximation, but less than the variance of the TWD given by either the "Saclay" or "modified Grenoble" approximations. This is reasonable; unlike the Gruber-Mullins Hamiltonian, Eq. (3) does not have fixed walls, so the steps can experience larger fluctuations. In spite of this, since the Gruber-Mullins approximation allows only one step to move, it can be regarded equally as an approximation for the TWD or for the SPD. The fact that the SPD is smaller than the other approximations of the TWD is apparently due to the fact that correlations between fluctuations of adjacent steps are to some degree taken into account in all these approximations, so that they are specifically approximations for the TWD, not the SPD.

Because the PEM confines both steps within a harmonic well, the theoretical asymptotic variance of the SPD must be finite. However, the vicinal surface is rough, and the variance of the SPD diverges logarithmically with the length of step Δy from which it is calculated. At some finite length L_W the prediction of the PEM is accurate. As Fig. 6 shows, $L_W \approx 14.2\xi_Q$. That so many "collisions" between neighboring steps are needed to adequately sample the statistics resulting from their interactions is supported by observations of the dependence of the TWD on Δy, as shown in Figs. 7–9.

In principle, the SPD could be used to determine $\widetilde{A}$. However, the SPD is strongly affected by the random position of the average step position, and it depends far too strongly on Δy. The TWD has neither of these two restrictions and is a more practical alternative for determining $\widetilde{A}$. Instead, the utility of the SPD lies in clarifying the PEM. The finite length L_W introduced in this work emerges more naturally than the finite length $\mathcal{V}$ that was introduced in Refs. 3 and 15, but the two are obviously related. Both help describe a short-lived dynamic constraint that is roughly analagous to a reptation tube[27] in polymer physics.

Naturally, the remarkable success of the PEM suggests that a Debye model[9] might lead to even better descriptions of vicinal crystal surfaces. Preliminary results[28] from such studies correctly show that $g_x(\Delta y)$ diverges logarithmically.

*Email address: amber_benson@yahoo.com

†Email address: Howard_Richards@tamu-commerce.edu; http://faculty.tamu-commerce.edu/HRichards/index.html

‡Email address: einstein@umd.edu; http://www2.physics.umd.edu/~einstein/

[1] F. Calogero, J. Math. Phys. **10**, 2191 (1969); **10**, 2197 (1969).

[2] B. Sutherland, J. Math. Phys. **12**, 246 (1971).

[3] H. L. Richards and T. L. Einstein, Phys. Rev. E **72**, 016124 (2005).

[4] M. Giesen and T. L. Einstein, Surf. Sci. **449**, 191 (2000).

[5] H. L. Richards, S. D. Cohen, T. L. Einstein, and M. Giesen, Surf. Sci. **453**, 59 (2000).

[6] T. L. Einstein, H. L. Richards, S. D. Cohen, and O. Pierre-Louis, Surf. Sci. **493**, 460 (2001).

[7] E. E. Gruber and W. W. Mullins, J. Phys. Chem. Solids **28**, 875 (1967).

[8] N. C. Bartelt, T. L. Einstein, and E. D. Williams, Surf. Sci. **240**, L591 (1990).

[9] See, e.g., N. W. Ashcroft and N. D. Mermin, *Solid State Physics* (Saunders College, Philadelphia, 1976), pp. 457–463.

[10] O. Pierre-Louis and C. Misbah, Phys. Rev. B **58**, 2259 (1998); **58**, 2276 (1998).

[11] T. Ihle, C. Misbah, and O. Pierre-Louis, Phys. Rev. B **58**, 2289 (1998).

[12] L. Masson, L. Barbier, J. Cousty, and B. Salanon, Surf. Sci. **317**, L1115 (1994).

[13] L. Barbier, L. Masson, J. Cousty, and B. Salanon, Surf. Sci. **345**, 197 (1996).

[14] E. L. Goff, L. Barbier, L. Masson, and B. Salanon, Surf. Sci. **432**, 139 (1999).

[15] J. A. Yancey, H. L. Richards, and T. L. Einstein, Surf. Sci. **598**, 78 (2005).

[16] B. P. Roe, *Probability and Statistics in Experimental Physics*, 2nd ed. (Springer, New York, 2001), pp. 7,8.

[17] N. C. Bartelt, T. L. Einstein, and E. D. Williams, Surf. Sci. **276**, 308 (1992).

[18] J. Villain and P. Bak, J. Phys. (Paris) **42**, 657 (1981).

[19] J. Villain, D. R. Grempel, and J. Lapujoulade, J. Phys. F: Met. Phys. **15**, 809 (1985).

[20] W. F. Saam, Phys. Rev. Lett. **62**, 2636 (1989).

[21] N. C. Bartelt, T. L. Einstein, and E. D. Williams, Surf. Sci. **224**, 149 (1991).

[22] H. Gebremariam, S. D. Cohen, H. L. Richards, and T. L. Einstein, Phys. Rev. B **69**, 125404 (2004).

[23] See, e.g., R. K. Pathria, *Statistical Mechanics*, 2nd ed. (Butterworth-Heinemann, Boston, 1996), pp. 30–40.

[24] T. L. Einstein and O. Pierre-Louis, Surf. Sci. **424**, L299 (1999).

[25] M. L. Mehta, *Random Matrices*, 2nd ed. (Academic, New York, 1991).

[26] F. Haake, *Quantum Signatures of Chaos* (Springer, Berlin, 1991).

[27] M. Doi and S. F. Edwards, *The Theory of Polymer Dynamics* (Clarendon, Oxford, 1986), pp. 189–217.

[28] C. A. Greene and H. L. Richards (unpublished).